

Study on feed-forward control of base-isolated buildings using predicted propagation of seismic waves



Ichiro Nagashima

Technology Center, Taisei Corporation, Japan

Ryota Maseki

Technology Center, Taisei Corporation, Japan

SUMMARY:

Two feed-forward control techniques for base-isolated buildings, in which the predicted propagation of seismic waves is used as input for control, are studied. One approach is a feed-forward control based on information about seismic motion obtained before its arrival. The empirical transfer function between two points along the propagation path of the seismic waves is used to predict the ground motion. A control algorithm using a limited period of the predicted ground motion is devised. The other approach is an optimal feedback control based on the state space equation of the entire augmented system, which includes the dynamics of the base-isolated building as well as the empirical transfer function of the seismic waves. The control performance of these two controls is compared and the effectiveness of the feed-forward control is confirmed. It is expected that this study will contribute to developing a new approach to feed-forward active control of building structures and equipment.

Keywords: Active response control, Feed-forward control, Feedback control, Prediction of ground motion

1. INTRODUCTION

Since an active mass driver system was first used on an actual Tokyo building in 1989 [Kobori et. al, 1991], there has been a steady increase in the number of buildings enhanced with active or semi-active response control systems in Japan. Active response control systems, and active mass damper systems in particular, have become firmly established as a technology that improves the habitability of super high-rise buildings during strong winds. Active response control systems are very effective. However, they use a feedback control law and are not suitable for controlling the seismic response of buildings due to limitations of control force and power. In other words, they are limited in application to the range from small to medium earthquakes.

This situation has led to considerable interest in semi-active response control systems, which offer the potential to control building response in the event of a major earthquake. Steady progress is being made with regard to practical applications of this technology [Kurata et. al. 1999, Yoshida 2001, Nagashima et. al. 2010].

This paper focuses on the use of feed-forward control techniques in base-isolated buildings to improve the control performance and efficiency of active response control systems. One approach to feed-forward control is to make use of predicted earthquake ground motion before its arrival. An empirical transfer function for seismic waves between two points along the propagation path is used; one at the point of prediction (the location of the control system) and the other closer to the hypocenter of the earthquake being predicted. This transfer function, which is referred to as the prediction filter [Nagashima et. al. 2008], is identified in the form of a state-space equation using past earthquake observations and is then used for the real-time prediction of future ground motions. When a 'target' earthquake occurs and the seismic waves reach the point near the hypocenter, the observed time-histories are used as the input to the state-space equation and ground motions at the control site are calculated in real time before the arrival of the actual motion. A control algorithm that uses such predicted ground motions of limited duration, which is several times the natural period of the base-isolated building, is presented.

Another approach is optimal feedback designed according to the state space equation of the entire augmented system, which includes the dynamics of the base-isolated building as well as the empirical transfer function of seismic wave propagation.

The control performance of these two control approaches is compared and the efficiency of feed-forward control is evaluated with respect to the required control force and energy.

2. LINEAR REGULATOR PROBLEMS WITH EXTERNAL EXCITATIONS

2.1. Optimal feedback and feed-forward control

To begin with, let us look back on the optimal control law for a class of optimal control problems – linear regulator problems with external excitations, following a variational approach [Kirk, D. E. 2004].

The plant is described by the linear state equations

$$\dot{\mathbf{x}}(t) = \mathbf{A}\mathbf{x}(t) + \mathbf{B}\mathbf{u}(t) + \mathbf{E}\ddot{\mathbf{z}}_0(t), \quad (2.1)$$

where \mathbf{A} and \mathbf{B} are $n \times n$ and $n \times m$ constant matrices, $\mathbf{x}(t)$ is the state vector, $\mathbf{u}(t)$ is the control input vector, and $\ddot{\mathbf{z}}_0(t)$ is the ground base acceleration.

The performance measure to be minimized is

$$\mathbf{J} = \frac{1}{2} \int_0^{t_f} \{ \mathbf{x}^T(t) \mathbf{Q} \mathbf{x}(t) + \mathbf{u}^T(t) \mathbf{R} \mathbf{u}(t) \} dt, \quad (2.2)$$

where \mathbf{Q} is a real symmetric positive semi-definite matrix and \mathbf{R} is real symmetric and positive definite. The final time t_f is fixed, $\mathbf{x}(t_f)$ is free, and the states and controls are not bounded.

The Hamiltonian is given by

$$H(\mathbf{x}(t), \mathbf{u}(t), \mathbf{p}(t), t) = \frac{1}{2} [\mathbf{x}^T(t) \mathbf{Q} \mathbf{x}(t) + \mathbf{u}^T(t) \mathbf{R} \mathbf{u}(t)] + \mathbf{p}^T(t) [\mathbf{A} \mathbf{x}(t) + \mathbf{B} \mathbf{u}(t) + \mathbf{E} \ddot{\mathbf{z}}_0(t)]. \quad (2.3)$$

The costate equations are

$$\dot{\mathbf{p}}(t) = - \frac{\partial H}{\partial \mathbf{x}} = - \mathbf{Q} \mathbf{x}(t) - \mathbf{A}^T \mathbf{p}(t) \quad (2.4)$$

and the algebraic relations that must be satisfied are given by

$$\mathbf{0} = \frac{\partial H}{\partial \mathbf{u}} = \mathbf{R} \mathbf{u}(t) + \mathbf{B}^T \mathbf{p}(t). \quad (2.5)$$

Therefore,

$$\mathbf{u}(t) = - \mathbf{R}^{-1} \mathbf{B}^T \mathbf{p}(t) \quad (2.6)$$

Let us assume that the costate is expressed by the equation

$$\mathbf{p}(t) = \mathbf{K}(t) \mathbf{x}(t) + \mathbf{s}(t) \quad (2.7)$$

Differentiating both sides with respect to t , we obtain

$$\dot{\mathbf{p}}(t) = \dot{\mathbf{K}}(t) \mathbf{x}(t) + \mathbf{K}(t) \dot{\mathbf{x}}(t) + \dot{\mathbf{s}}(t).$$

Substituting from Eq. (2.4) for $\dot{\mathbf{p}}(t)$, and Eq. (2.1) for $\dot{\mathbf{x}}(t)$, and using Eq. (2.7) to eliminate $\mathbf{p}(t)$, we obtain

$$\begin{aligned} & [\dot{\mathbf{K}}(t) + \mathbf{Q} + \mathbf{K}(t) \mathbf{A} + \mathbf{A}^T \mathbf{K}(t) - \mathbf{K}(t) \mathbf{B} \mathbf{R}^{-1}(t) \mathbf{B}^T \mathbf{K}(t)] \mathbf{x}(t) \\ & + [\dot{\mathbf{s}}(t) + \mathbf{A} \mathbf{s}(t) - \mathbf{K}(t) \mathbf{B} \mathbf{R}^{-1} \mathbf{B}^T \mathbf{s}(t) + \mathbf{K}(t) \mathbf{E} \ddot{\mathbf{z}}_0(t)] = \mathbf{0} \end{aligned} \quad (2.8)$$

Because this must be satisfied for all $\mathbf{x}(t)$ and $\mathbf{s}(t)$, we obtain

$$\dot{\mathbf{K}}(t) = - \mathbf{K}(t) \mathbf{A} - \mathbf{A}^T \mathbf{K}(t) - \mathbf{Q} + \mathbf{K}(t) \mathbf{B} \mathbf{R}^{-1} \mathbf{B} \mathbf{K}(t) \quad (2.9)$$

and

$$\dot{\mathbf{s}}(t) = - [\mathbf{A}^T - \mathbf{K}(t) \mathbf{B} \mathbf{R}^{-1} \mathbf{B}] \mathbf{s}(t) - \mathbf{K}(t) \mathbf{E} \ddot{\mathbf{z}}_0(t) \quad (2.10)$$

To obtain the boundary conditions we have, from Eq. (2.7),

$$\mathbf{p}(t_f) = \mathbf{K}(t_f) \mathbf{x}(t_f) + \mathbf{s}(t_f) = \mathbf{0}. \quad (2.11)$$

Since this equation must be satisfied for all $\mathbf{x}(t_f)$, the boundary conditions are

$$\mathbf{K}(t_f) = \mathbf{0}, \text{ and } \mathbf{s}(t_f) = \mathbf{0} \quad (2.12)$$

In the following study, a constant matrix \mathbf{K} , which is obtained for an infinite-time process as $t_f \rightarrow \infty$, is used to determine the feedback control force. The \mathbf{K} matrix is obtained by solving the algebraic matrix Riccati equation

$$\mathbf{0} = -\mathbf{K}\mathbf{A} - \mathbf{A}^T \mathbf{K} - \mathbf{Q} + \mathbf{K}\mathbf{B}\mathbf{R}^{-1} \mathbf{B}^T \mathbf{K}, \quad (2.13)$$

obtained by setting $\dot{\mathbf{K}}(t) = \mathbf{0}$ in Eq. (2.9).

The optimal feedback and feed-forward control force is the sum of the optimal feedback control force $\mathbf{u}_{fb}(t)$ ($= -\mathbf{R}^{-1} \mathbf{B}^T \mathbf{K} \mathbf{x}(t)$) and the optimal feed-forward control force $\mathbf{u}_{ff}(t)$ ($= -\mathbf{R}^{-1} \mathbf{B}^T \mathbf{s}(t)$):

$$\mathbf{u}(t) = \mathbf{u}_{fb}(t) + \mathbf{u}_{ff}(t) = -\mathbf{R}^{-1} \mathbf{B}^T \mathbf{K} \mathbf{x}(t) - \mathbf{R}^{-1} \mathbf{B}^T \mathbf{s}(t). \quad (2.14)$$

Substituting Eq. (2.14) into Eq. (2.1), we obtain

$$\dot{\mathbf{x}}(t) = \mathbf{A}_c \mathbf{x}(t) + \mathbf{F} \mathbf{s}(t) + \mathbf{E} \ddot{\mathbf{z}}_0(t), \quad (2.15)$$

where $\mathbf{F} = -\mathbf{R}^{-1} \mathbf{B}^T$ and $\mathbf{A}_c = \mathbf{A} - \mathbf{R}^{-1} \mathbf{B}^T \mathbf{K}$.

The state space equation for $\mathbf{s}(t)$, which determines the feed-forward control force, is expressed by

$$\dot{\mathbf{s}}(t) = -\mathbf{A}_c^T \mathbf{s}(t) - \mathbf{K} \mathbf{E} \ddot{\mathbf{z}}_0(t). \quad (2.16)$$

To predict the input base acceleration $\ddot{\mathbf{z}}_0(t)$, we introduce the following identified state space equations, which as noted above are known as the prediction filter [Nagashima et. al. 2008]:

$$\dot{\mathbf{z}}_d(t) = \mathbf{A}_d \mathbf{z}_d(t) + \mathbf{D}_d \ddot{\mathbf{w}}(t), \quad \ddot{\mathbf{z}}_0(t) = \mathbf{C}_d \mathbf{z}_d(t), \quad (2.17)$$

where $\ddot{\mathbf{w}}(t)$ is the input acceleration to the prediction filter.

Once $\ddot{\mathbf{z}}_0(t)$ is predicted with the help of Eq. (2.17), the optimal feed-forward control force may be calculated by integrating Eq. (2.16) backward in time starting from $t = t_f$. It is generally believed that the whole time history of the input base acceleration should be known beforehand in order to determine the feed-forward control force. A control algorithm using the predicted base acceleration of limited duration will be considered and presented later.

To study the frequency response characteristics of the feedback and feed-forward control with respect to the accelerations input into the prediction filter, an extended state space equation is defined from Eqs. (2.15), (2.16) and (2.17) as follows:

$$\begin{pmatrix} \dot{\mathbf{x}}(t) \\ \dot{\mathbf{s}}(t) \\ \dot{\mathbf{z}}_d(t) \end{pmatrix} = \begin{bmatrix} \mathbf{A}_c & \mathbf{F} & \mathbf{E} \mathbf{C}_d \\ \mathbf{0} & -\mathbf{A}_c^T & \mathbf{K} \mathbf{E} \mathbf{C}_d \\ \mathbf{0} & \mathbf{0} & \mathbf{A}_d \end{bmatrix} \begin{pmatrix} \mathbf{x}(t) \\ \mathbf{s}(t) \\ \mathbf{z}_d(t) \end{pmatrix} + \begin{pmatrix} \mathbf{0} \\ \mathbf{0} \\ \mathbf{D}_d \end{pmatrix} \ddot{\mathbf{w}}(t) \quad (2.18)$$

2.2. Optimal feedback control considering dynamics of prediction filter

Next, an optimal feedback control is designed based on the state space equation of the entire augmented system, which includes the dynamics of the base-isolated building as well as the prediction filter (the empirical transfer function of seismic wave propagation).

From Eqs. (2.1) and (2.17), the state space equation for the entire augmented system is established as follows:

$$\dot{\mathbf{x}}_E(t) = \mathbf{A}_E \mathbf{x}_E(t) + \mathbf{B}_E \mathbf{u}(t) + \mathbf{E}_E \ddot{\mathbf{w}}(t) \quad (2.19)$$

where

$$\mathbf{x}_E(t) = \begin{pmatrix} \mathbf{x}(t) \\ \mathbf{z}_d(t) \end{pmatrix}, \quad \mathbf{A}_E = \begin{bmatrix} \mathbf{A} & \mathbf{E} \mathbf{C}_d \\ \mathbf{0} & \mathbf{A}_d \end{bmatrix}, \quad \mathbf{B}_E = \begin{pmatrix} \mathbf{B} \\ \mathbf{0} \end{pmatrix} \text{ and } \mathbf{E}_E = \begin{pmatrix} \mathbf{0} \\ \mathbf{D}_d \end{pmatrix}.$$

The performance measure to be minimized is

$$\mathbf{J}_E = \frac{1}{2} \int_0^{t_f} \left\{ \mathbf{x}_E^T(t) \mathbf{Q}_E \mathbf{x}_E(t) + \mathbf{u}_E^T(t) \mathbf{R}_E \mathbf{u}_E(t) \right\} dt \quad (2.20)$$

where \mathbf{Q}_E is a real symmetric positive semi-definite matrix and \mathbf{R}_E is real symmetric and positive definite.

The optimal feedback control force $\mathbf{u}_E(t)$ is obtained as

$$\mathbf{u}_E(t) = -\mathbf{R}_E^{-1} \mathbf{B}_E^T \mathbf{K}_E \mathbf{x}_E(t), \quad (2.21)$$

where \mathbf{K}_E is the solution of the following algebraic matrix Riccati equation

$$\mathbf{0} = -\mathbf{K}_E \mathbf{A}_E - \mathbf{A}_E^T \mathbf{K}_E - \mathbf{Q}_E + \mathbf{K}_E \mathbf{B}_E \mathbf{R}_E^{-1} \mathbf{B}_E^T \mathbf{K}_E \quad (2.22)$$

As is clear from Eq. (2.21), the effects of the ground base accelerations are considered in the feedback control force.

3. FUNDAMENTAL STUDY ON FREQUENCY RESPONSE CHARACTERISTICS

3.1. Analysis model

Let us consider a single-degree-of-freedom building model. The mass, the stiffness and the natural frequency of the building model are denoted by m_s , k_s , ω_s , respectively. The damping coefficient and the corresponding damping factor are denoted by c_s and ζ_s . The displacement of the structure x_s is relative to the ground. The scalar control force and the ground base acceleration are given by $u(t)$ and $\ddot{z}_0(t)$, respectively.

The state space equations are given by Eq. (2.1), where $\mathbf{x}(t) = (x_s(t), \dot{x}_s(t))$,

$$\mathbf{A} = \begin{bmatrix} 0 & 1 \\ -\omega_s^2 & -2\zeta_s \omega_s \end{bmatrix}, \quad \mathbf{B} = \begin{bmatrix} 0 \\ m_s^{-1} \end{bmatrix}, \quad \mathbf{E} = \begin{bmatrix} 0 \\ -1 \end{bmatrix}, \quad \omega_s = \sqrt{\frac{k_s}{m_s}}, \quad \zeta_s = \frac{c_s}{2m_s \omega_s} \quad (3.1)$$

The performance measure is given by Eq. (2.2), where

$$\mathbf{Q} = \begin{bmatrix} q_1 \\ q_2 \end{bmatrix}, \quad \mathbf{R} = [r] \quad (3.2)$$

The solution of the matrix Riccati equations are given by $\mathbf{K} = \begin{bmatrix} k_{11} & k_{12} \\ k_{12} & k_{22} \end{bmatrix}$,

where $k_{11} = 2\zeta_s \omega_s k_{12} + \omega_s^2 k_{22} + k_{12} k_{22} / (m_s^2 r)$, $k_{12} = -m_s^2 r \omega_s^2 + \sqrt{m_s^4 r^2 \omega_s^4 + m_s^2 r q_1}$ and

$$k_{22} = -2m_s^2 r \zeta_s \omega_s + \sqrt{4m_s^4 r^2 \zeta_s^2 \omega_s^2}$$

Next, the prediction filter is simplified as a band pass filter, of which the transfer function is

$$\frac{\ddot{z}_0(s)}{\ddot{w}(s)} = \frac{\omega_d^2}{s^2 + 2\zeta_d \omega_d s + \omega_d^2} \cdot \frac{s^2}{s^2 + 2\zeta_h \omega_h s + \omega_h^2}. \quad (3.3)$$

The corresponding state space equation is given by (2.19), where

$$\mathbf{A}_d = \begin{bmatrix} 0 & 1 & 0 & 0 \\ 0 & 0 & 1 & 0 \\ 0 & 0 & 0 & 1 \\ -a & -b & -c & -d \end{bmatrix}, \quad \mathbf{D}_d = \begin{bmatrix} 0 \\ 0 \\ 0 \\ \omega_d^2 \end{bmatrix}, \quad \mathbf{C}_d = \begin{bmatrix} 0 \\ 0 \\ 1 \\ 0 \end{bmatrix}^T, \quad \mathbf{z}_d = \begin{bmatrix} z_0 \\ \dot{z}_0 \\ \ddot{z}_0 \\ \ddot{\ddot{z}}_0 \end{bmatrix} \quad (3.4)$$

$$a = \omega_d^2 \omega_h^2, \quad b = 2\omega_d \omega_h (\zeta_d \omega_h + \zeta_h \omega_d), \quad c = \omega_d^2 + 4\zeta_d \zeta_h \omega_d \omega_h + \omega_h^2, \quad d = 2(\zeta_h \omega_h + \zeta_d \omega_d).$$

3.2. Comparison of control performance in the frequency domain

The frequency responses of the optimal feedback and feed-forward control (FBFFC) presented in section 2.1, as well as those of the optimal feedback control (FBC) presented in section 2.2, with respect to the input acceleration $\ddot{w}(i\omega)$ are calculated from the Fourier transform of Eq. (2.18) and Eq. (2.19), respectively. The parameters for the building model are as follows: $\omega_s = 2\pi$ rad/s, $\zeta_s = 0.01$ and $m_s = 1.0$ kg. The parameters for the prediction filter are; $\omega_h = \omega_s / 10$, $\zeta_h = 0.70$, $\omega_d = 10 \times \omega_s$ and $\zeta_d = 0.707$. Figure 3.1. shows the frequency response function of the prediction filter.

Figure 3.2.(a) shows an example of the frequency responses of the building velocity per unit input acceleration with FBFFC compared with those with FBC. The dimensionless weighting parameters for the control are defined as $r, \bar{q}_1 = q_1 / (m_s^2 \omega_s^4 r)$ and $\bar{q}_2 = q_2 / (m_s^2 \omega_s^2 r)$. The frequency responses are calculated for the combinations $\bar{q}_1 = \bar{q}_2 = 1 \times 10^{-1}$ and 0 (i.e. no control) with $r = 1.0$. The equivalent modal damping factor of the building is increased to 21.7% by the feedback control. The corresponding frequency responses of the control forces per unit input acceleration are shown in Figure 3.2.(b). The velocity response with FBFFC is remarkably decreased and the required control force is less than with FBC.

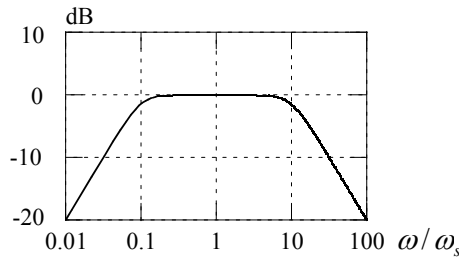
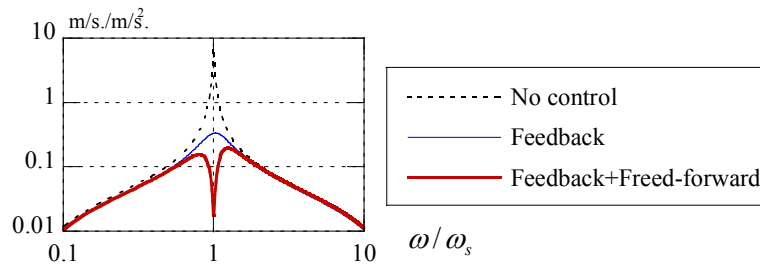
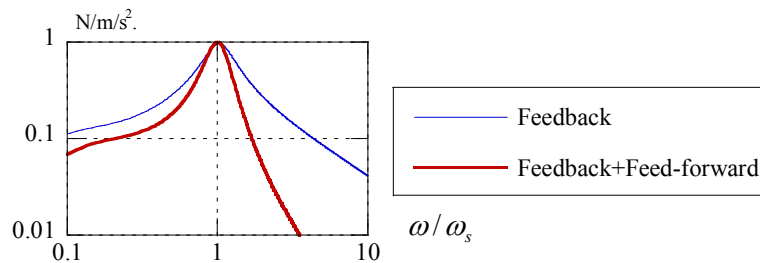


Figure 3.1. Frequency response function of prediction filter



(a) Velocity of building



(b) Control force

Figure 3.2. Frequency responses per unit input acceleration

4. ALGORITHM TO DETERMINE FEED-FORWARD CONTROL FORCE

It is rather easy to study the control performance of FBFFC in the frequency domain, as presented in chapter 3. To evaluate the optimal feed-forward control force in the time domain, it is necessary in general to know the whole time history of the ground base accelerations in advance [Sato 1990]. To evaluate the feed-forward control force, a control algorithm that uses the free vibration component that can be predicted in advance has been presented [Naraoka 1992]. A control algorithm that uses the limited duration of the input accelerations has been devised based on the dynamic programming approach [Kawahara 1989]. However, there appears to be no fully developed practical control algorithm to determine the feed-forward control force in the time domain. In the sections that follow, an optimal feed forward control that uses the whole time history is first considered, then a practical control algorithm approximating the optimal feed-forward control force based on the input base

acceleration of limited duration will be presented.

4.1. Optimal feed-forward control with global optimization

The impulse response function of the feed-forward control force may be calculated using Eq. (2.16) backward in time starting from $t = t_f$, where $\ddot{\mathbf{z}}_0(t)$ is replaced by the Dirac delta function $\delta(t)$ as follows:

$$\dot{\mathbf{s}}(t) = -\mathbf{A}_c^T \mathbf{s}(t) - \mathbf{K}\mathbf{E}\delta(t) \quad (4.1)$$

Let us assume that the transition matrix of the state space equation (4.1) is $\Phi(t)$. The impulse response function $\mathbf{h}(t)$, which is an anti-causal function, is then obtained by

$$\left. \begin{aligned} \mathbf{h}(t) &= \mathbf{0} && \text{for } t > 0 \\ \mathbf{h}(t) &= -\Phi(t)\mathbf{K}\mathbf{E}\{1\} && \text{for } t \leq 0 \end{aligned} \right\} \quad (4.2)$$

where $\Phi(t)$ is calculated from the inverse Laplace transform of the transfer function $(s\mathbf{I} + \mathbf{A}_c^T)^{-1}$.

The feed-forward control force at time t may be given by

$$\mathbf{u}_{ff}(t) = -\mathbf{R}^{-1}\mathbf{B}^T \mathbf{s}(t_f - t), \quad (4.3)$$

where $\mathbf{s}(t)$ is calculated backward in time by the following equation,

$$\mathbf{s}(t_f - t) = \Phi(t - t_f) \cdot \mathbf{s}(t_f) - \int_{t_f}^t \mathbf{h}(t - \tau) \ddot{\mathbf{z}}_0(\tau) d\tau. \quad t_f \geq t \geq 0 \quad (4.4)$$

The second term on the right-hand side of Eq. (4.4) is a convolution integral. Assuming the boundary condition $\mathbf{s}(t_f) = \mathbf{0}$, Eq.(4.4) is simplified as

$$\mathbf{s}(t_f - t) = -\int_{t_f}^t \mathbf{h}(t - \tau) \ddot{\mathbf{z}}_0(\tau) d\tau \quad (4.5)$$

As is clear from Eq. (4.5), the full time history of the ground base acceleration from t_f to t must be known in advance to determine the feed-forward control force at t .

Let us divide the time history of the ground base acceleration into N blocks with each endpoint of an interval denoted by $t_i, (i = 1, \dots, N)$.

The feed-forward control force for the i -th block may be calculated by

$$\mathbf{u}_{ffi}(t) = -\mathbf{R}^{-1}\mathbf{B}^T \mathbf{s}(t_i - t) \quad (4.6)$$

where $\mathbf{s}(t_i - t)$ is evaluated, following Eqs. (4.4) and (4.5), as

$$\mathbf{s}(t_i - t) = \Phi(t - t_i) \cdot \mathbf{s}(t_f - t_i) - \int_{t_i}^t \mathbf{h}(t - \tau) \ddot{\mathbf{z}}_0(\tau) d\tau \quad t_i \geq t \geq t_{i-1} \quad (4.7)$$

and

$$\mathbf{s}(t_f - t_i) = -\int_{t_f}^{t_i} \mathbf{h}(t - \tau) \ddot{\mathbf{z}}_0(\tau) d\tau \quad (4.8)$$

The feed-forward control force for the i -th block is determined by Eq. (4.6), which we call the feed-forward control by global optimization (GFFC).

4.2. Optimal feed-forward control with individual optimization

Next, let us consider the following individual performance measure:

$$\mathbf{J}_i = \frac{1}{2} \int_{t_{i-1}}^{t_i} \{ \mathbf{x}^T(t) \mathbf{Q} \mathbf{x}(t) + \mathbf{u}^T(t) \mathbf{R} \mathbf{u}(t) \} dt, \quad (4.9)$$

where the ground base acceleration is assumed to be zero after t_i (or the boundary condition $\mathbf{s}(t_i) = \mathbf{0}$ is assumed). The optimal feed-forward control force for the i -th block may be calculated using Eq. (4.5):

$$\hat{\mathbf{u}}_{ffi}(t) = -\mathbf{R}^{-1}\mathbf{B}^T \hat{\mathbf{s}}(t_i - t) \quad (4.10)$$

where

$$\hat{\mathbf{s}}(t_i - t) = -\int_{t_i}^t \mathbf{h}(t - \tau) \ddot{\mathbf{z}}_0(\tau) d\tau \quad t_i \geq t \geq t_{i-1} \quad (4.11)$$

The feed-forward control force for the i -th block is determined by Eq. (4.10), which we call the feed-forward control by individual optimization (IFFC). The GFFC is expected to perform better than the IFFC, due to the effect of the first term on the right-hand side of Eq. (4.4), i.e. the homogeneous solution, which, however, may be negligible as long as $|t - t_i|$ is sufficiently large that the transition matrix $\Phi(t - t_i)$ approaches $\mathbf{0}$.

If the homogeneous solution becomes small enough for $t_i - t \geq T_d$ and the ground base acceleration can be predicted for more than $T_d + T_a$ seconds in advance, the IFFC $\hat{\mathbf{u}}_{ff_i}(t)$ may approximate to the GFFC $\mathbf{u}_{ff_i}(t)$ for t ranging between t_{i-1} and $t_{i-1} + T_a$. Using this principle, a control algorithm to improve the performance of IFFC is devised as shown in Figure 4.1., where the IFFC $\hat{\mathbf{u}}_{ff_i}(t)$ of the coming $T_d + T_a$ seconds is calculated at $t = t_{i-1}$ and used for T_a seconds; the IFFC $\hat{\mathbf{u}}_{ff_{i+1}}(t)$ of the coming $T_d + T_a$ seconds is calculated at $t = t_i (= t_{i-1} + T_a)$ and used for T_a seconds; feed-forward control forces are determined by incrementally repeating this procedure, which we call the feed-forward control by modified individual optimization (MIFFC).

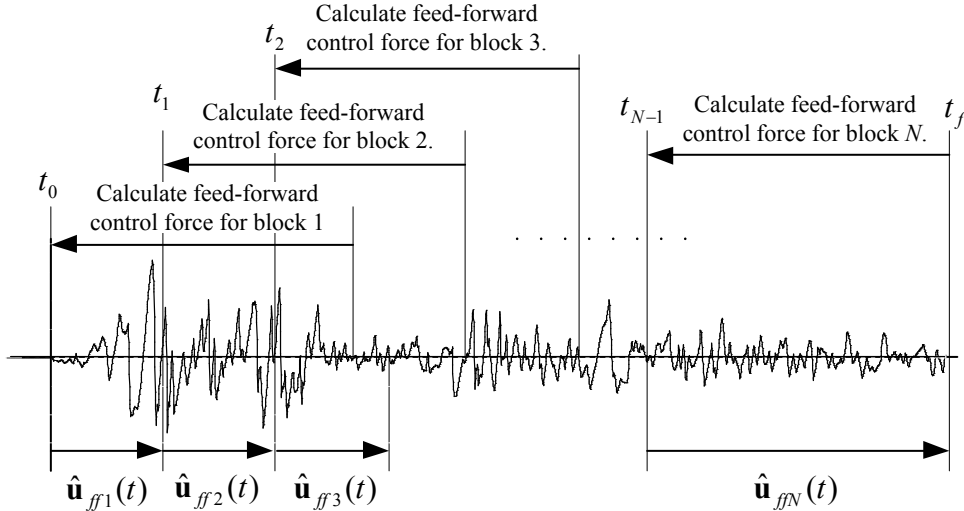


Figure 4.1. Schematic for determining the **feed-forward** control force for MIFFC

5. CONTROL PERFORMANCE IN TIME DOMAIN

5.1. Analysis model

Let us consider a single-degree-of-freedom building model. The parameters for the building model and the prediction filters are the same as those presented in section 3.1. The transition matrix of the state space equation (4.1) is expressed as

$$\Phi(t) = e^{h_c \omega_c t} \begin{bmatrix} \cos \alpha t - \frac{h_c \omega_c}{\alpha} \sin \alpha t & \frac{\omega_c^2}{\alpha} \sin \alpha t \\ -\frac{1}{\alpha} \sin \alpha t & \cos \alpha t + \frac{h_c \omega_c}{\alpha} \sin \alpha t \end{bmatrix} \quad (5.1)$$

where $\alpha = \omega_c \sqrt{1 - h_c^2}$, $\omega_c^2 = \omega_s^2 + \frac{k_{12}}{m_s^2 r}$ and $2h_c \omega_c = 2h_s \omega_s + \frac{k_{22}}{m_s^2 r}$.

5.2. Comparison of control performance in the time domain

A modified sinusoidal wave with a frequency of ω_s is used as the input acceleration, with the peak acceleration scaled to 1.0 m/s. The same control parameters as described in section 3.2 are used. The velocity responses with the FBFFC are calculated, where the GFFC or the IFFC is used to obtain the feed-forward control force. The responses with the FBC as presented in section 2.2 are also calculated for comparison. The input acceleration and the responses are shown in Figure 5.1. The input acceleration is divided into three blocks for calculation of the feed-forward control force for IFFC; each block has a duration of four seconds.

Figure 5.1.(c) shows that the velocity response of the building with FBFFC (GFFC) is reduced significantly compared to that with FBC, using almost the same amount of control force. The velocity response with FBFFC (IFFC) is not as good as that with FBFFC(GFFC), but still far better than with FBC. The difference in control force between FBFFC (IFFC) and FBFFC (GFFC) is due to the homogeneous solution, as pointed out in section 4.2.

To improve the performance of IFFC, MIFFC is studied, where the feed-forward control force is calculated for the four seconds of each block and the first one second is used for control. The responses with FBFFC (MIFFC) are compared with those using FBFFC (GFFC) and FBFFC (IFFC) in Figure 5.2. The feed-forward control force for IFFC is zero at each block endpoint (at four, eight and twelve seconds) as shown in Figure 5.2.(b), which causes control performance degradation. The feed-forward control force for MIFFC coincides with that for GFFC. As a result, MIFFC successfully maintains control performance that is as good as GFFC.

To investigate the control performance of FBFFC (MIFFC) under the influence of earthquake excitations, the N-S component of the 18 May 1940 El-Centro Earthquake, shown in Figure 5.3., is scaled to a peak ground acceleration (PGA) of 1.0m/s and used as the input acceleration. The dimensionless weighting parameters are assigned as $\bar{q}_1 = \bar{q}_2 = 1 \times 10^{-1}$ and $\bar{q}_1 = \bar{q}_2 = 5 \times 10^{-1}$ with $r = 1.0$ for FBC and FBFFC (MIFFC), respectively, such that the maximum control forces are comparable. The equivalent modal damping factors are increased to 21.7% and 44.1% for FBC and FBFFC (MIFFC), respectively.

The maximum velocity responses for FBC and FBFFC(MIFFC) are 0.135m/s and 0.059m/s, respectively, while the corresponding maximum control forces are 0.386N and 0.354N, respectively. The maximum control power for FBFFC(MIFFC) is 0.016W, which is less than the 0.051W for FBC.

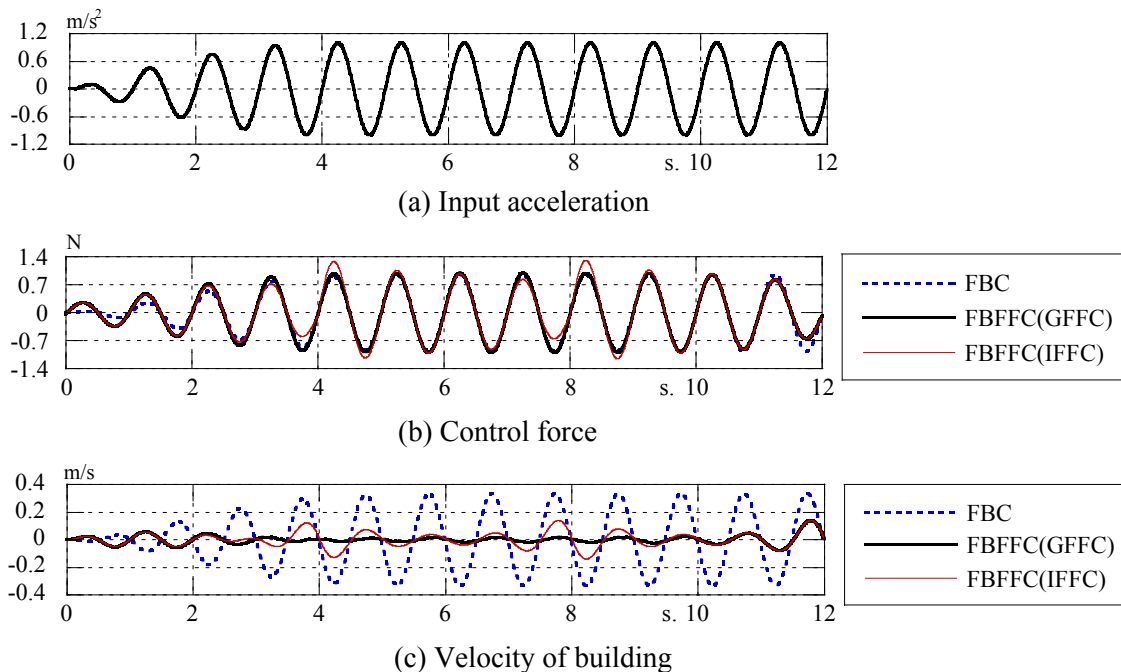


Figure 5.1. Comparison of responses with FBC and FBFFC

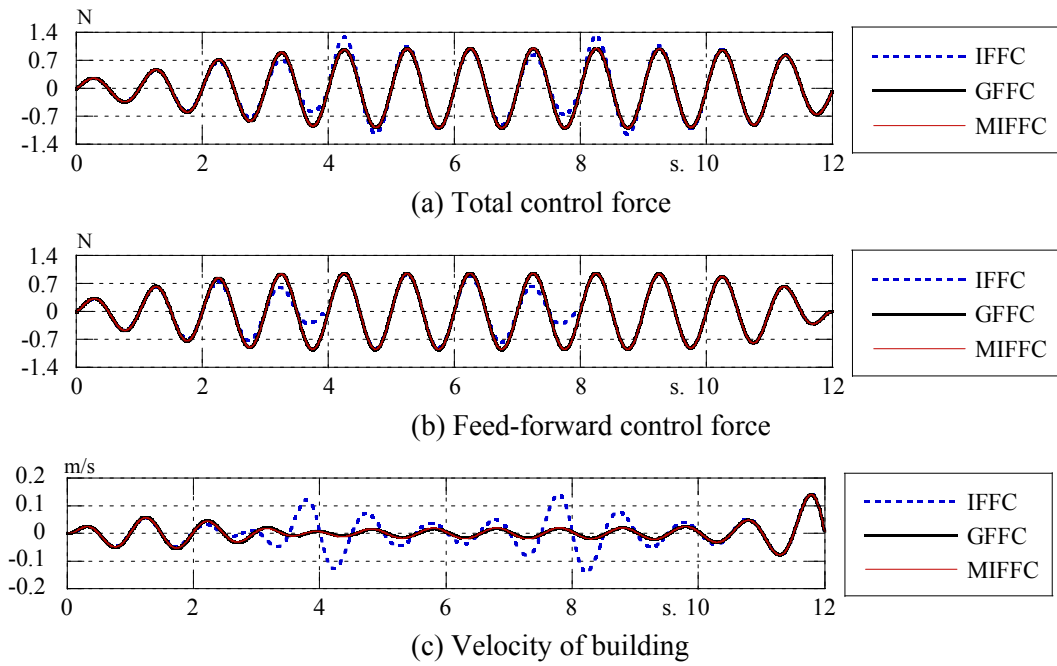


Figure 5.2. Comparison of responses with FBFFC

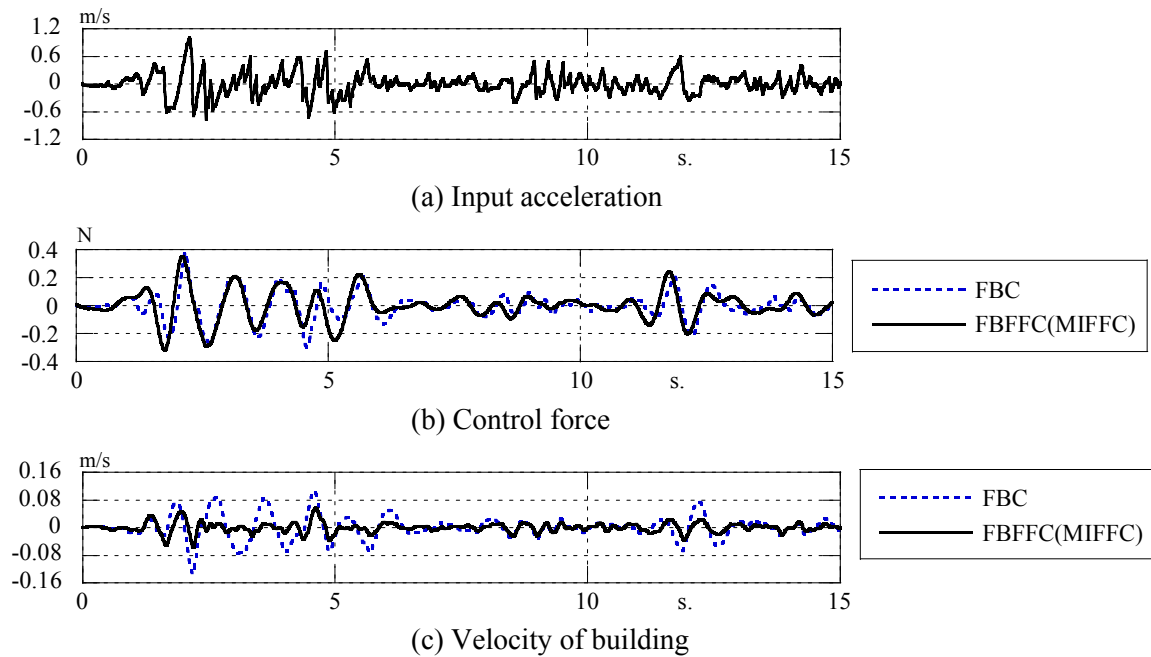


Figure 5.3. Comparison of earthquake responses with FBFFC

6. CONCLUSIONS

The authors present an investigation of feed-forward control techniques for base-isolated buildings in which the predicted propagation of seismic waves is used as the input for control. An empirical transfer function between two points along the seismic wave propagation path is used to predict the ground base acceleration in advance. Feed-forward control forces are then calculated backward in time using the limited-duration predictions of ground motions and the first few seconds of the resulting control force, which are free from homogeneous solutions, are used for control. The analysis

demonstrates that it is not necessary to have available the whole time history of ground base acceleration in order to determine the feed-forward control force.

Through numerical examples, it is demonstrated that optimal feedback and feed-forward control (FBFFC) performs better than optimal feedback control (FBC); FBFFC reduces building response drastically compared with FBC with the same amount of control force.

ACKNOWLEDGEMENT

This research was partially supported by JSPS Grant-in-Aid for challenging Exploratory Research (22651067).

REFERENCES

- Kawahara, M. and Fukazawa, K. (1989). Optimal control of structure subject to earthquake loading using dynamic programming. *Proc. of JSCE*, No.404/i-11, 179s-190s.
- Kirk, D. E. (2004). Optimal control theory, an introduction, Dover Publications, Inc. Mineola, New York.
- Kobori, T., Koshika, N., Yamada, K. and Ikeda, Y. (1991). Seismic-response-controlled structure with active mass driver system. Part 1: design. *Earthquake Engng. Struct. Dyn.* **20**, 133-149.
- Kurata N., Kobori T., Takahashi M., Niwa N., and Midorikawa H. (1999). Actual seismic response controlled building with semi-active damper system. *Earthquake Engineering and Structural Dynamics*, **28**, 1427-1447.
- Nagashima, I., Yoshimura, C., Uchiyama, Y., Maseki, R. and Itoi, T. (2008). Real-time prediction of earthquake ground motion using empirical transfer function. *Proc. of 14th WCEE*, **S02-023**.
- Nagashima, I., Shinozaki, Y., Maseki, R., Sanui, Y. and Kitagawa, Y. (2010). Sliding mode control of base-isolation system using semi-active hydraulic damper. *J. Struct. Constr. Eng., AIJ*, **Vol.75 No.649**, 511-519. (in Japanese)
- Naraoka K. and Katukura, H. (1992). A study on feedback-feedforward control algorithm which utilizes information of future input. *J. Struct. Constr. Eng., AIJ*, **No.438**, 75-81. (in Japanese)
- Sato Y., Ishimaru, S. and Miwa, S. (1989). Comparative study for control algorithm of SDOF structures, Part II On procedures for tracking problems. *AIJ annual meeting*, 549-550. (in Japanese)
- Yoshida, K. (2001). First building with semi-active base isolation. *Journal of Japan Society of Mechanical Engineers*, **Vol.104, No.995**, 48-52. (in Japanese)